

**Modelling
wave–current
interactions off the
east coast of
Scotland**

A. D. Sabatino et al.

This discussion paper is/has been under review for the journal Ocean Science (OS).
Please refer to the corresponding final paper in OS if available.

Modelling wave–current interactions off the east coast of Scotland

A. D. Sabatino¹, C. McCaig^{1,a}, R. B. O’Hara Murray², and M. R. Heath¹

¹Marine Population Modelling Group, Department of Mathematics and Statistics, University of Strathclyde, Glasgow, UK

²Marine Scotland Science, Marine Laboratory, Aberdeen, UK

^anow at: Brookes Bell, 280 St Vincent Street, Glasgow, UK

Received: 20 November 2015 – Accepted: 9 December 2015 – Published: 18 December 2015

Correspondence to: A. D. Sabatino (alessandro.sabatino@strath.ac.uk)

Published by Copernicus Publications on behalf of the European Geosciences Union.

Title Page

Abstract

Introduction

Conclusions

References

Tables

Figures

◀

▶

◀

▶

Back

Close

Full Screen / Esc

Printer-friendly Version

Interactive Discussion

Abstract

Densely populated coastal areas of the North Sea are particularly vulnerable to severe wave conditions, which overtop or damage sea-defences leading to dangerous flooding. Around the shallow southern North Sea, where the coastal margin is low-lying and population density is high, oceanographic modelling has helped to develop forecasting systems to predict flood risk. However coastal areas of the deeper northern North Sea are also subject to regular storm damage but there has been little or no effort to develop coastal wave models for these waters. Here we present a high spatial resolution model of northeast Scottish coastal waters, simulating waves and the effect of tidal currents on wave propagation, driven by global ocean tides, far-field wave conditions, and local air pressure and wind stress. We show that the wave–current interactions and wave–wave interactions are particularly important for simulating the wave conditions close to the coast at various locations. The model can simulate the extreme conditions experienced when high (spring) tides are combined with sea-level surges and large Atlantic swell. Such a combination of extremes represents a high risk for damaging conditions along the Scottish coast.

1 Introduction

Due to its semi-enclosed morphology and shoaling bathymetry, the North Sea experiences extreme wave conditions, in particular during winter periods (Woolf et al., 2002). When combined with sealevel surges such events can lead to damaging inundation of low-lying coastal regions, due to wave-overtopping of sea-defences. Development of a modelling and predictive capability for high resolution wave conditions in the North Sea is therefore a high priority. However the task is complicated due to interaction between locally-generated waves and incoming swell from outside the region, and, especially, due to interactions between waves and tidal currents.

OSD

12, 3099–3142, 2015

Modelling wave–current interactions off the east coast of Scotland

A. D. Sabatino et al.

Title Page

Abstract

Introduction

Conclusions

References

Tables

Figures

◀

▶

◀

▶

Back

Close

Full Screen / Esc

Printer-friendly Version

Interactive Discussion



Modelling wave–current interactions off the east coast of Scotland

A. D. Sabatino et al.

Title Page

Abstract

Introduction

Conclusions

References

Tables

Figures

◀

▶

◀

▶

Back

Close

Full Screen / Esc

Printer-friendly Version

Interactive Discussion



Crossing, or bi-modal sea states occur between 5 and 40 % of the time in the North Sea (Guedes Soares, 1984). These are generated when swell waves propagating into the region from distant storm events interact with locally-generated waves which may be of very different direction, period and height. Swell waves from the North Atlantic and Norwegian Sea propagate into the North Sea, interacting with local windsea generated waves, modifying the main spectral parameters. The interaction between differing wave-trains is not fully understood, but crossing seas have been statistically associated with freak wave incidence, and shipping accidents (Waseda et al., 2011; Tamura et al., 2009; Cavaleri et al., 2012; Onorato et al., 2006, 2010; Sabatino and Serio, 2015; Tofoli et al., 2011). The North Sea is particularly prone to rogue wave events, such as the famous Draupner Wave recorded in 1994 (Haver, 2004), the first ever recorded rogue wave event, that occurred in crossing sea conditions (Adcock et al., 2011).

In addition to crossing seas, wave–current interactions are a well known cause of wave height amplification or attenuation. Wave–currents interactions (WCI) are depth- and current-induced modification of wave features. A seminal study carried out by Tolman (1991) highlighted that wave–current interactions are significant in the North Sea, changing the significant wave height (H_s) and the mean wave period (T_m) by 5 and 10 % respectively during storm periods. However the model that was used by Tolman (1991) to assess this effect, was at very coarse resolution and broad scale. In particular the effect of the WCI in the coastal shallow areas was not considered. Phillips (1977) showed that in the absence of wave-breaking, local wave amplitude is given by:

$$\frac{A}{A_0} = \frac{c_0}{\sqrt{c(c + 2U)}} \quad (1)$$

where A is the resulting wave amplitude, A_0 is the unperturbed amplitude of the wave field, c is the wave phase speed, and U is the current that interacts with the wave train. It is important to notice that the sign of the current is determinant on the effect of the WCI: if the current travels in opposite direction with the wave train, there will be an enhancement of the significant wave height. Conversely if current and waves are in the

Modelling wave–current interactions off the east coast of Scotland

A. D. Sabatino et al.

Title Page

Abstract

Introduction

Conclusions

References

Tables

Figures

◀

▶

◀

▶

Back

Close

Full Screen / Esc

Printer-friendly Version

Interactive Discussion



same direction, the H_s decreases. For deep water waves, the phase speed, c , depends only on the period of the wave, while in shallow water c depends only on the depth. Equation (1) shows that the waves travelling in a direction opposing the current ($U < 0$) have a positive ratio A/A_0 and, consequently, an enhancement of the wave amplitude.

Wave–current interactions could also lead to the breaking of the wave: if the current is strong enough to block the wave train (Ris and Holthuijsen, 1996), these waves can break and lose energy before arriving to the coastline (Chawla and Kirby, 2002, 1998).

WCI are particularly difficult to quantify empirically, and computationally intensive to model. However, it is clear that shallow coastal waters, embayments and headlands are particular foci for interactions (Hearn et al., 1987; Signell et al., 1990). Model studies have concentrated on comparing wave height and period in coupled and uncoupled model versions showing, for example, 3% difference in wave height and 20% in wave period in the Dutch and German coastal waters of the North Sea (Osuna and Monbaliu, 2004). Similar results have been obtained for coastal waters of the Adriatic during Bora conditions (Benetazzo et al., 2013), finding a maximum reduction for the H_s of 0.6 m in the central Adriatic and a simultaneous increase up to 0.5 m in Trieste and Venice Gulf. WCI were also studied during hurricane conditions off the eastern seaboard of the USA (Xie et al., 2008).

Sea defences of coastal settlements along the northeast coast of Scotland have suffered several damaging events during the period 2009–2014 as a result of surge and wave. The coastal waters are dominated by strong tidal currents and wind-driven residuals, and are exposed to wave trains entering the North Sea from the north, and generated by storm events in the central and southern North Sea. Although the oceanography of the North Sea as a whole has been intensively studied since the 1830s (Whewell, 1830; Proudman and Doodson, 1924; Dietrich, 1950; Huthnance, 1991; Otto et al., 1990), and the region was one of the earliest to be subjected to computational hydrodynamic modelling (Flather, 1987; Davies et al., 1985), high resolution modelling activity has been largely concentrated in areas with potential for wave and tidal energy extraction (Adcock et al., 2013; Bryden and Couch, 2006; Baston and

Modelling wave–current interactions off the east coast of Scotland

A. D. Sabatino et al.

Title Page

Abstract

Introduction

Conclusions

References

Tables

Figures

◀

▶

◀

▶

Back

Close

Full Screen / Esc

Printer-friendly Version

Interactive Discussion



Harris, 2011; Shields et al., 2011, 2009). However, there are no such models for the northeast coast of mainland Scotland, and none which include coupled wave–current interactions. Our objective here was to develop and test such a model for the stretch of coastline between the Firth of Tay and Peterhead, centred on the strategically important port-city of Aberdeen and the town of Stonehaven (Fig. 1). The latter is the base for a governmentally supported marine monitoring site with $a > 15$ year time series of high resolution data on a wide range of environmental parameters (Bresnan et al., 2009).

2 Materials and methods

The MIKE by DHI model was used to simulate the tidal-, wind-driven circulation, and the wave propagation. The MIKE software is composed of different modules, for the creation of a model grid and input files and to simulate different hydrodynamical features at the same time or separately. The following modules were used:

- the MIKE ZERO modules for generating the computational grid and the input files
- the MIKE 3 FM module for simulating the tidal and the wind-driven circulation
- the MIKE 21 SW module for modelling the wave propagation.

For the simulation of the wave–current interactions a one way coupling between MIKE 3 FM and MIKE 21 SW was setup. The depth average flow fields and the water level output from MIKE 3 FM was provided as input to the MIKE 21 SW model.

2.1 The computational grid

Both MIKE 3 FM and MIKE 21 SW use an unstructured grid approach, with triangular elements (Ferziger and Perić, 2002). Unstructured grids can represent complex coastlines better than a rectangular grid and potentially provide more realistic flows, enabling the geography of the coastline to affect the propagation of tidal and surface

Modelling wave–current interactions off the east coast of Scotland

A. D. Sabatino et al.

Title Page

Abstract

Introduction

Conclusions

References

Tables

Figures

◀

▶

◀

▶

Back

Close

Full Screen / Esc

Printer-friendly Version

Interactive Discussion



waves in a realistic manner. In addition, triangular grid elements allow smoothly changing cell sizes across a region, with the highest resolution concentrated in an area of particular interest. The mesh for the area of study is shown in Fig. 2. An enhanced resolution area was created near Stonehaven, because this work is part of a wider study focusing on the resuspension of the sediments in this part of the domain. This high resolution area also covered the Firth of Forth and the Aberdeenshire coastline, where previous studies have shown to be enhanced currents due to interaction between the tidal wave and the Scottish coastline (Dietrich, 1950; Otto et al., 1990).

2.2 The MIKE 3FM hydrodynamic model

MIKE 3FM (Flow Model) is based on the numerical solution of the 3-D incompressible Reynolds averaged Navier–Stokes equations, under the Boussinesq and the hydrostatic pressure approximations (DHI, 2011a). The spatial discretization of the primitive equations is performed using a cell-centered finite-volume method. In the finite-volume method the volume integrals in the partial differential equations with a divergence are converted to surface integrals using the Gauss–Ostrogradsky theorem (Toro, 2009).

MIKE 3 FM has a flexible approach for simulating the flow in the water column. It is possible to choose between sigma layers (Song and Haidvogel, 1994), z layers and a coupled sigma and z layers. For our purpose we decided to use the equidistant sigma layers approach, because the bathymetry of the area was not sufficiently complex to require a more accurate description with a coupled sigma and z layer that would be extremely computationally expensive. Sigma layers are also useful for resolving the water column well throughout the tidal cycle, given the large tidal range. The coupled sigma- and z layers were tested, but there was no significant improvement for simulating the flow.

For the Horizontal Eddy Viscosity the formulation proposed by Smagorinsky (1963) was used, in which the sub-grid scale transport is expressed by an effective eddy viscosity related to a characteristic length scale rather than a constant eddy viscosity. This

sub-grid scale viscosity is given by

$$A = c_s^2 l^2 \sqrt{2S_{ij}S_{ij}} \quad (2)$$

where c_s is the Smagorinsky constant, l is the characteristic length of the grid size and the deformation rate is given by (Lilly, 1966; Deardorff, 1971; Smagorinsky, 1963)

$$S_{ij} = \frac{1}{2} \left(\frac{\partial u_i}{\partial x_j} + \frac{\partial u_j}{\partial x_i} \right). \quad (3)$$

The Smagorinsky constant was set to 0.2.

The bed resistance was parametrized using a constant quadratic drag coefficient c_f . The average bottom stress is determined by a quadratic friction law:

$$\bar{\tau}_b = c_f \rho_0 \bar{u}_b |\bar{u}_b| \quad (4)$$

where \bar{u}_b is the average flow velocity above the bottom and ρ_0 is the density of the water. The drag coefficient was set as $c_f = 0.0025$.

The model was forced with a time series of tidal elevations at the open boundaries from the open-source OSU (Oregon State University) Tidal Prediction Software (OTPS) (Egbert et al., 2010), based on TOPEX satellite observation of the water level observations interpolated with tide gauge data from the European shelf region. In order to take account of the wind-driven circulation and surge in the model, meteorological forcing were applied across the model domain, using the ERA-Interim reanalysis for wind velocity and mean sea level pressure (Dee et al., 2011).

2.3 The MIKE 21SW wave model

The MIKE 21 SW (Spectral Wave) is an unstructured grid model for wave prediction and analysis (DHI, 2011b). The MIKE 21 SW is based on the wave action conservation equation (Komen et al., 1996; Young, 1999), where the dependent variable is the

directional-frequency wave action spectrum.

$$\frac{\partial N}{\partial t} + \nabla \cdot (cN) = \frac{S}{\sigma} \quad (5)$$

where S is the energy source term, defined as

$$S = S_{\text{in}} + S_{\text{nl}} + S_{\text{ds}} + S_{\text{bot}} + S_{\text{surf}} \quad (6)$$

5 that depends on the energy transfer from the wind to the wave field S_{in} , on the non-linear wave-wave interaction S_{nl} , on the dissipation due to depth induced wave breaking S_{surf} , on the dissipation due to bottom friction S_{bot} , and on the dissipation caused by the white-capping S_{ds} .

10 The wave action density spectrum $N(\sigma, \theta)$ is defined as (Bretherton and Garrett, 1968):

$$N(\sigma, \theta) = \frac{E(\sigma, \theta)}{\sigma} \quad (7)$$

15 where E is the wave energy density spectrum, $\sigma = 2\pi f$ is the angular frequency (where f is the frequency), and θ is the direction of wave propagation. The momentum transfer from the wind to the waves follows the formulation in Komen et al. (1996). The momentum transfer and the drag depend not only on the strength of the wind but also on the wave state itself. The roughness is specified with the Charnock parameter (0.01).

For the physics of the propagation and breaking of the waves we choose the following parameters:

- The depth-induced wave breaking is based on the formulation of Battjes and Janssen (1978), in which the gamma parameter is a constant 0.6 across the domain. The formulation of the depth-induced wave breaking can be written as:

$$S_{\text{surf}}(\sigma, \theta) = -\frac{\alpha Q_b \bar{\sigma} H_m^2}{8\pi} \frac{E(\sigma, \theta)}{E_{\text{tot}}} \quad (8)$$

Modelling wave–current interactions off the east coast of Scotland

A. D. Sabatino et al.

Title Page

Abstract

Introduction

Conclusions

References

Tables

Figures

◀

▶

◀

▶

Back

Close

Full Screen / Esc

Printer-friendly Version

Interactive Discussion



where $\alpha \approx 1.0$ is a calibration constant, Q_b is the fraction of breaking waves, $\bar{\sigma}$ is the spectrum average frequency, E_{tot} is the total wave energy that is linked to the wave action density spectrum, and H_m is the estimated maximum wave height, that is defined as $H_m = \gamma d$ (Battjes and Janssen, 1978), in which d is the depth and γ is the free breaking parameter (Battjes, 1974) fixed, after the calibration, as 0.6.

- The bottom friction is specified in the model as the Nikuradze roughness (k_N) (Nikuradse, 1933; Johnson and Kofoed-Hansen, 2000) with $k_N = 0.01$ m.
- The white capping formulation described in Komen et al. (1996) in order to consider the dissipation of waves, based on the theory of Hasselmann (1974). For the fully spectral formulation, the white capping assumes a form that is dependent on the mean frequency $\bar{\sigma}$ and on the wavenumber k :

$$S_{\text{ds}}(\sigma, \theta) = -C_{\text{ds}} \left(\bar{k}^2 m_0 \right)^2 \left[(1 - \delta) \frac{k}{\bar{k}} + \delta \left(\frac{k}{\bar{k}} \right)^2 \right] \bar{\sigma} N(\sigma, \theta). \quad (9)$$

here the two parameters C_{ds} and δ are the two dissipation coefficients, that control the overall dissipation rate and the strength of dissipation in the energy/action spectrum respectively, and m_0 is the zeroth moment of the overall spectrum. After the calibration, we chose to use $C_{\text{ds}} = 2$ and $\delta = 0.8$.

The forcings included in the model are the local wind and the swell wave field from outside the model area and specified at the model boundaries. For the model boundaries we used boundary conditions from the Venugopal and Nemalidine (2014, 2015) North Atlantic model, a larger wave model that encompass the Southern Norwegian Sea and the North Atlantic Ocean. The ERA-Interim $0.125^\circ \times 0.125^\circ$ model was used to provide a wind field across the model domain with a time resolution of 6 h (Dee et al., 2011; Berrisford et al., 2011).

2.4 Validation data sets

The model was validated using five independent data-sets. The hydrodynamic model was validated using data from the UK National Tide Gauge Network in Aberdeen and Leith and using the tide gauge data from the Scottish Environmental Protection Agency (SEPA) in Buckie. Validation was performed comparing harmonic components extracted from time-series of both model and real data. The harmonic components of the sealevel were extracted using the UTide Matlab function (Codiga, 2011).

Current meter observations from the British Oceanographic Data Centre (BODC) were used to validate the modelled currents. For the wave model we compared recorded data from wave gauges in the Moray Firth and in the Firth of Forth (obtained from CEFAS) and data from a wave rider buoy deployed in Aberdeen Bay (data obtained from University of Aberdeen). In addition, we used significant wave height and mean wave period from satellite data provided by WaveNet (CEFAS) for June 2008. Expecially important in this case is the Aberdeen wave gauge, since this is the only one in shallow water (the depth of the sea in the mooring location is 10 m). This allow us to evaluate the ability of the model in coastal areas, in which the wave-currents interactions are strongest.

Table 1 shows details of the observations used for validating and calibrating the tidal and wave model, while in Fig. S1 in the Supplement we show the position of the tide and wave gauges used for the validation and the position of the satellite data.

The validation for waves was carried out using four statistical indices: the bias, the Root-Mean Square error (RMSE), the correlation coefficient (R) and the Scatter Index (SI). These indices are defined below

$$\text{Bias} = \frac{1}{N} \sum_{i=1}^N (x_{o_i} - x_{m_i}) \quad (10)$$

OSD

12, 3099–3142, 2015

Modelling wave–current interactions off the east coast of Scotland

A. D. Sabatino et al.

Title Page

Abstract

Introduction

Conclusions

References

Tables

Figures

◀

▶

◀

▶

Back

Close

Full Screen / Esc

Printer-friendly Version

Interactive Discussion



$$\text{RMSE} = \sqrt{\frac{1}{N} \sum_{i=1}^N (x_{o_i} - x_{m_i})^2} \quad (11)$$

$$R = \frac{\sum_{i=1}^N (x_{o_i} - \bar{x}_o) (x_{m_i} - \bar{x}_m)}{\sqrt{\sum_{i=1}^N (x_{o_i} - \bar{x}_o)^2 (x_{m_i} - \bar{x}_m)^2}} \quad (12)$$

$$\text{SI} = \frac{\text{RMSE}}{\bar{x}_o} \quad (13)$$

5 For tidal current validation we used, instead of the SI, the Normalized RMS error (NRMSE), that is defined as:

$$\text{NRMSE} = \frac{\text{RMSE}}{\max(x) - \min(x)} \quad (14)$$

10 The validation was performed for different years: for the hydrodynamic model the agreement between modelled and observed water level was evaluated for the entire 2007, while the currents were validated for 1992, where the rotor current meter observations were available. The wave model was validated for 2010 and for 2008, where observations and boundary inputs were available.

3 Results

3.1 Validation of the hydrodynamic model

15 The hydrodynamic model was calibrated for the 2007, based on the agreement with the recorded water level at the tide gauge in Aberdeen. After calibration, the MIKE 3

Modelling wave–current interactions off the east coast of Scotland

A. D. Sabatino et al.

Title Page

Abstract

Introduction

Conclusions

References

Tables

Figures

◀

▶

◀

▶

Back

Close

Full Screen / Esc

Printer-friendly Version

Interactive Discussion



tidal model was validated against harmonic components extracted from both observed and modelled data for water level. The agreement between modelled and observed currents was also investigated. Root Mean Square Error (RMSE) for the amplitude and the phase of harmonic components was less than 10 % for all the cases. In particular for the dominant M_2 component, the phase error was very low and the amplitude was well modelled (see Table 2 and Table S1 in the Supplement for more details). The validation results show that the modelled results are in a good agreement with the recorded tidal amplitude and phase. The model was run for 1992 and measurements obtained from BODC from eight locations were used to validate the currents in the model. The validation of the single components u and v is reported in Table S2 in the Supplement. Table 3 shows that the model adequately represent the current speeds in the domain. The validation shows that that the model slightly underestimate the current, however it can be noticed that the bias of the model was very low. The RMS error, except for one observation, does not exceed percentually the 15 % of the maximum speed.

3.2 Validation of the wave model

The results of the wave gauges and satellite validation are reported in Table 4. We evaluated the performance of the wave model with wave–current interactions implemented (coupled) and without WCI (uncoupled). There was a good agreement between modelled with WCI and measured wave data. The bias does not exceed 0.15 m for significant wave height. Table 4 and Fig. 3 shows that the model estimates correctly the significant wave height in the Firth of Forth and in Aberdeen, but underestimates this parameter in the Moray Firth. However the agreement with the data is still satisfactory. In particular low RMSE values were recorded for the Aberdeen wave gauge, that is the only coastal shallow-water wave gauge that is available in the area (the depth of the mooring site is 10 m). The model performance against satellite data randomly sampled throughout the domain shows a good agreement. Without the WCI included in the model, small or no differences were estimated for significant wave height, but larger differences were seen for mean wave periods (the calculated RMSE for the un-

Modelling wave–current interactions off the east coast of Scotland

A. D. Sabatino et al.

Title Page

Abstract

Introduction

Conclusions

References

Tables

Figures

◀

▶

◀

▶

Back

Close

Full Screen / Esc

Printer-friendly Version

Interactive Discussion



coupled model was 0.97 s in Aberdeen, 1.24 s in the Firth of Forth and 1.83 s in the Moray Firth). Comparing satellite observations in spring and winter conditions, it is possible to conclude that, in general, the model provides accurate predictions for wave heights $< 1.5\text{--}2$ m, but slightly underestimates the height of larger waves. On the other hand, wave periods are better modelled in winter period, where the waves are higher. No or very small differences were recorded between coupled and uncoupled model for satellite validation. This because the resolution of the satellite data is low and because the satellite data are often in deep water, where the WCI are less important.

3.3 Wave–current interaction

Predicted wave field with and without wave–current interaction were compared during a 7 month period in 2010, covering both winter and summer conditions, for evaluating the importance of WCI on wave features. The results are shown in Fig. 4. For the comparison between the coupled and the uncoupled model the Root Mean Square (RMS) between the two runs was computed. Results show some differences between the two runs, in particular, the largest deviations, due to WCI, are found in coastal areas, such as around headlands, bays and in estuaries, in which the currents (mostly driven by tides) are strongest. As expected the highest differences were seen in the proximity of the coastline (Signell et al., 1990): this was because the strength of the currents (mainly tidal-driven) are stronger (Dietrich, 1950; Otto et al., 1990). During spring tides, higher values for the current were recorded off Northeast England and near Peterhead and Aberdeen (see Fig. 1). Wave periods are more affected than wave heights in this coupling, with RMS deviations that can be on average of 20 % (absolute value) in shallow-water coastal areas. We also considered the effect of the wave–current interactions on the wave directional spreading, as this is an important variable for the stability of the wave train in deep water and on its evolution (Benjamin and Feir, 1967). The results showed that during the 7 month period the significant wave height was, on average, less affected than directional spreading or wave periods: the difference was of the order of magnitude of 0.1 m near the coastline and less offshore, while the difference

in peak spectral wave period (T_p) exceeded 1 s in some of the east coast Firths such as the Moray Firth and the Firth of Forth. The maximum variation of H_s between the coupled and the uncoupled run was +3 and -2 m, both occurring during storm events.

3.4 Current and swell effect on the wind-sea wave field

In order to study the importance of the wave-current interactions and the coupling between swell and wind-sea waves off the east coast of Scotland, three storms were considered in the period January–August 2010. Storm events were identified by examining the time series in the Firth of Forth and the Moray Firth in which the highest H_s were recorded. These three storms were selected because they were the three most intense storms during the considered period and originated from different weather conditions.

3.4.1 The 26–27 February 2010 storm

Between the 25–27 February 2010, the UK was affected by a low pressure system, that moved rapidly from west to east. From the afternoon of the 25th to the 26th the centre of the storm was over the North Sea (Fig. 5). At the same time, another low pressure system (not shown in the map) was over the Norwegian Sea, causing a train of swell moving from N to S. The low pressure over North Sea caused windsea waves exceeding 4 m. In Fig. 6 the situation in the sea is showed at 12:30 UTC of the 26th: swell waves contributed to enhancing the H_s in the centre of the storm, while a train of swell waves was forming from this storm, travelling west to the Moray Firth. Interaction of the windsea and the swell waves caused high waves along the east coast: the maximum recorded H_s by the Firth of Forth wave gauge was 4.8 m. WCI contributed to the enhancement of H_s by up to 1 m in coastal areas, while in the open sea the contribution was very low, up to 0.1 m. In the afternoon of the 26th (Fig. 7, at 19:00 p.m.) the storm was near the Firth of Forth. The contribution of the swell waves was significant, increasing the H_s by up to 1 m: model outputs showed that the central part of the storm had a $H_s > 5$ m, while without the swell coming from North the centre of the storm would

Modelling wave-current interactions off the east coast of Scotland

A. D. Sabatino et al.

Title Page

Abstract

Introduction

Conclusions

References

Tables

Figures

◀

▶

◀

▶

Back

Close

Full Screen / Esc

Printer-friendly Version

Interactive Discussion



have been an $H_s < 4.5$ m. To our knowledge no significant damages were recorded for this storm.

3.4.2 The 30–31 March 2010 storm

The larger storm in 2010 occurred during the night of 30 March 2010. Between 29 March 2010 and 1 April 2010 the SE coast of Scotland and the north of England was struck by severe weather and very strong winds. These conditions were caused by a strong depression that originated from a weak minimum near the Azores Islands, in the North Atlantic, in front of the Portuguese coast. This low pressure was < 990 hPa once over Great Britain and Ireland at midnight of the 30 March 2010 and reached its minimum the day after with a depression of < 980 hPa over the North of England. The evolution of the storm from surface pressure charts from ECMWF ERA-Interim reanalysis is reported in Fig. 8 (Dee et al., 2011; Berrisford et al., 2011). These figures clearly show that the depression, at its maximum strength, is just above the S of Scotland during the night between the 30–31 March 2010. This depression generated both very high waves (H_s exceeded 6 m, measured in the Firth of Forth) and surge waves exceeding 0.5 m (measured both by Aberdeen and Leith tide gauges). The waves caused significant damages to the coastal defences of cities in the SE of Scotland. In particular the City of Edinburgh council estimated the damages to coastal defences to be about GBP 23 000. Also in Berwick at the southern entrance of the Firth of Forth some damages were caused to the harbour infrastructures. To the east, in Dumbar waves topped the roof of 2-floor houses.

Damaging conditions associated with this storm were caused by a combination of simultaneous factors: (1) tides in the spring period, (2) a surge wave of about 0.5 m generated by local pressure and wind, (3) wind-sea waves generated locally that were interacting with strong currents, (4) a weak, but significant, swell waves field, interacted with the windsea waves.

Modelling wave–current interactions off the east coast of Scotland

A. D. Sabatino et al.

Title Page

Abstract

Introduction

Conclusions

References

Tables

Figures

◀

▶

◀

▶

Back

Close

Full Screen / Esc

Printer-friendly Version

Interactive Discussion



Figure 9 shows the intensity of the current in Aberdeen wave gauge location and the resulting wave–current interaction. It can be seen that the current was strongly enhanced by the wind, and, consequently the WCI effect was stronger.

At about 00:30 a.m. on 31 March 2010 the storm was at its maximum causing the wave field to hit the coastline at around the same time as high tide and surge. The different components of the storm were analyzed. First, the surge wave generated by the minimum of pressure above the North Sea was studied. Figure 10 shows the difference between the total water level and the water level due to tides at 02:00 UTC on 31 March 2015. The model predicted a surge wave up to 0.5 m. A comparison between the recorded water level and the model output showed that the model underestimated the surge wave by about 0.1 m. The reason of this underestimation could be because the boundary conditions for the model only included tidal water level and did not include the surge wave from outside the model. The surge wave extended from the Firth of Forth southwards: the water level in those regions was enhanced the water level by about 0.4–0.5 m. In addition to these surge conditions, the H_s of the waves at the same time were exceeding 7 m in the same areas (see Figs. 11 and 12). Figures 11 and 12 show the wave field at two different times at the storm, at 00:30 a.m., and at 02:00 a.m. respectively. The swell waves effect was very low, but contributed to the enhancement of H_s up to 0.5 m, while on the coastline the contribution of the WCI was very strong. At 02:00 UTC on 31 March 2010 (Fig. 12), when the storm reaches the coastline, WCI increased H_s by up to 2.5 m in many locations near the Firth of Forth (see Fig. 12d). Figures 11f and 12f show a high H_s swell waves at the entrance of the Firth of Forth. These were waves generated by the large storm shown in Fig. 11e, but are no longer influenced by the local wind, but are propagating outside the centre of the windsea waves to the coastline. H_s recorded by the Firth of Forth wave gauge measured a peak of significant wave height of 6.46 m at 05:00 UTC on 31 March 2015. The model matched the peak recorded in the wave gauge reasonably well, predicting higher values S of the Firth of Forth, where more damages were caused.

Modelling wave–current interactions off the east coast of Scotland

A. D. Sabatino et al.

[Title Page](#)[Abstract](#)[Introduction](#)[Conclusions](#)[References](#)[Tables](#)[Figures](#)[◀](#)[▶](#)[◀](#)[▶](#)[Back](#)[Close](#)[Full Screen / Esc](#)[Printer-friendly Version](#)[Interactive Discussion](#)

3.4.3 The 19 June 2010 storm

The third storm that is considered in this paper was one that generated high off-shore waves conditions, with swell propagating to the coastline. This is an example of how the coupling of swell and windsea waves could lead to extreme wave conditions, with significant wave height exceeding 6 m offshore and 4–5 m on the coastline. Figure 13 shows the pressure conditions between the 18–20 June 2010. On the 17 June 2010 (not shown) a system of low pressure was generated between Greenland and Iceland. This minimum moved quickly to the Scandinavian peninsula, intensifying and remaining in the area of Sweden and Norway for 72 h. This low pressure caused strong winds in the northern North Sea and consequently the generation of waves in the area between the Norway and Scotland. This field of waves arrived at the Scottish coastline at the same time as the low pressure was generating high waves in the bulk of the North Sea, causing two trains of waves to be in the same place at the same time. This condition, known as crossing or bimodal sea, is quite common in the North Sea (Guedes Soares, 1984). The model hindcasted that the storm offshore was at its maximum near 16:00 UTC of the 19 June 2010 (Fig. 14). At 16:00 UTC on 19 June 2010 the modelled offshore, mid North Sea, windsea generated waves peaked at $H_s \sim 5$ m (Fig. 14e), whereas the swell waves were a little smaller with $H_s \sim 3$ –4 m (Fig. 14f). Further north, in the Moray Firth, the swell waves dominated with the swell having $H_s \sim 6$ m and the windsea having $H_s \sim 2$ m. The resulting predicted wave field had $H_s > 6$ m (Fig. 14b). In the Moray Firth H_s of more than 5 m was recorded. However, at this time, the coupling between currents and wave caused a decrease of the significant wave height at the coastline (Fig. 14c). In some locations H_s was reduced by more than 0.5 m (see Fig. 14c and d). 3 h later (Fig. 15), the turning tidal currents enhanced the waves by more than 1.5 m in coastal locations. Figure 3 shows that the model matches almost perfectly the water level recorded in the Moray Firth and in the Firth of Forth wave gauges at this time.

4 Conclusions

In this study we presented a model capable of hindcasting surge and storms in the east coast of Scotland. The combination of spring tide, strong wind and high waves can be extremely threatening in coastal areas. The North Sea is one of the areas most affected by this forcings. Storms in North Sea can generate extremely high waves as well as rogue waves (Ponce de León and Guedes Soares, 2014).

Results indicate that wave–currents and wave–wave interactions play a fundamental role in the wave climate. The validation shows that the model performs reasonably well during both calm periods and storms for waves, and also performs well for tides and surges.

During severe storms, in particular when the low pressure was over England and Scotland, was found that the wave–current interactions (WCI) are significant, causing an increase, or decrease, in H_s that can exceed 2 m in some coastal areas, depending on the direction of the wave field compared to the current. A similar result was found for the peak spectral wave period: Fig. 4 shows that in the time period considered here the largest deviation of wave periods due to WCI is in the estuarine areas of the east coast, with average deviations more of than 1.2 s.

Wave propagation in the Firth of Forth during storms generated in the mid-North Sea is driven by trains of swell waves detaching from the open-sea storm. During the stormy periods considered here, the windsea waves in the Firth of Forth did not exceeded 3.5 m in the outer area of the estuary and 1 m in the inner part, while the swell field exceeded 5 m at the entrance of the Firth of Forth. In the inner Firth the swell waves have a similar magnitude to the windsea waves. Conversely, the area of the estuary of the Forth is mainly driven by locally generated waves. A similar behavior was noticed in the other two estuarine areas on the east coast: the Tay estuary and the Moray Firth.

The north-east coast of Scotland is more exposed to swell arriving from the North Atlantic and the Norwegian Sea, while the central and the southern part is more exposed to local windsea waves and to storms generated in the bulk of the North Sea.

OSD

12, 3099–3142, 2015

Modelling wave–current interactions off the east coast of Scotland

A. D. Sabatino et al.

Title Page

Abstract

Introduction

Conclusions

References

Tables

Figures

◀

▶

◀

▶

Back

Close

Full Screen / Esc

Printer-friendly Version

Interactive Discussion



Modelling wave–current interactions off the east coast of Scotland

A. D. Sabatino et al.

Title Page

Abstract

Introduction

Conclusions

References

Tables

Figures

◀

▶

◀

▶

Back

Close

Full Screen / Esc

Printer-friendly Version

Interactive Discussion



The model also has forecasting capabilities, in particular when nested with large scale models, such as the North Atlantic model (Venugopal and Nemalidine, 2015, 2014). A limitation of the model is that the MIKE by DHI software does not allow an on-line coupling between waves and tides, slowing the simulation process. In fact, currents and waves are simulated by different modules and is not possible to perform a direct coupling. For this work the currents were simulated first and then the output were saved in order to use them as input for the wave model. Another limitation of the model, due to the one-way coupling, is that we can not study the effect of the wave set-up and set-down on the surge water level (Longuet-Higgins and Stewart, 1962; Bowen et al., 1968). However, this can be implemented in the future, running first the wave model, then using the wave radiation in the hydrodynamic model, to estimate the enhancement of the water level due to waves near the shoreline.

This research also underlines the importance of high-resolution regional scale models for the understanding of sea dynamics and for the forecasting of dangerous sea states: larger models usually have inadequate resolution to estimate the effect of such processes near the coastline. Future work will be focused on the hindcasting of freakish wave state based on the estimation of the kurtosis from the parameters of the model (Janssen, 2003; Tamura et al., 2009; Ponce de León and Guedes Soares, 2014) and on the sediments resuspension in the area of Stonehaven (Heath et al., 2015), which is an intensive study site for suspended sediment and other biological variables in the water column (Serpetti et al., 2011, 2012).

The Supplement related to this article is available online at doi:10.5194/osd-12-3099-2015-supplement.

Acknowledgements. The authors wish to acknowledge Ian Thurlbeck, Robert Wilson, Alessandra Romanó, Reddy Nemaliddine, Vengatesan Venugopal, Jon Side, Arne Vogler, Ruari MacIver and Simon Waldman for their helpful suggestions. The authors are grateful for the financial support of the UK Engineering and Physical Sciences Research Council (EPSRC)

through the TeraWatt-Large scale Interactive coupled 3-D modelling for wave and tidal energy resource and environmental impact consortium (EPSRC Grant Ref: EP/J010170/1). The authors are also grateful to Cefas (UK) for providing satellite and wave gauges data, to Thomas O'Donoghue for providing Aberdeen bay wave buoy data, to the British Oceanographic Data Center (BODC) and the Scottish Environmental Protection Agency (SEPA) for the tide gauge and RCM data, and to the European Centre for Medium-Range Weather Forecasts (ECMWF) for providing wind and pressure data.

References

- Adcock, T., Taylor, P., Yan, S., Ma, Q., and Janssen, P.: Did the Draupner wave occur in a crossing sea?, *P. Roy. Soc. Lond. A Mat.*, 467, 3004–3021, 2011. 3101
- Adcock, T. A., Draper, S., Houlby, G. T., Borthwick, A. G., and Serhadlioglu, S.: The available power from tidal stream turbines in the Pentland Firth, *P. Roy. Soc. Lond. A Mat.*, 469, 20130072, doi:10.1098/rspa.2013.0072, 2013. 3102
- Baston, S. and Harris, R.: Modelling the hydrodynamic characteristics of tidal flow in the Pentland Firth, in: *EWTEC 2011*, 5–9 September 2011, Southampton, UK, 1–7, 2011. 3102
- Battjes, J.: Surf similarity, *Coast. Engin. Proc.*, 1, 466–480, 1974. 3107
- Battjes, J. and Janssen, J.: Energy loss and set-up due to breaking of random waves, *Coast. Engin. Proc.*, 1, 569–587, 1978. 3106, 3107
- Benetazzo, A., Carniel, S., Sclavo, M., and Bergamasco, A.: Wave–current interaction: effect on the wave field in a semi-enclosed basin, *Ocean Model.*, 70, 152–165, 2013. 3102
- Benjamin, B. T. and Feir, J.: The disintegration of wave train on deep water, *J. Fluid Mech.*, 7, 417–430, 1967. 3111
- Berrisford, P., Kållberg, P., Kobayashi, S., Dee, D., Uppala, S., Simmons, A., Poli, P., and Sato, H.: Atmospheric conservation properties in ERA-Interim, *Q. J. Roy. Meteor. Soc.*, 137, 1381–1399, 2011. 3107, 3113
- Bowen, A. J., Inman, D. L., and Simmons, V. P.: Wave “set-down” and set-Up, *J. Geophys. Res.*, 73, 2569–2577, doi:10.1029/JB073i008p02569, doi:10.1029/JB073i008p02569, 1968. 3117
- Bresnan, E., Hay, S., Hughes, S., Fraser, S., Rasmussen, J., Webster, L., Slesser, G., Dunn, J., and Heath, M.: Seasonal and interannual variation in the phytoplankton community in the north east of Scotland, *J. Sea Res.*, 61, 17–25, 2009. 3103

Modelling wave–current interactions off the east coast of Scotland

A. D. Sabatino et al.

Title Page

Abstract

Introduction

Conclusions

References

Tables

Figures

◀

▶

◀

▶

Back

Close

Full Screen / Esc

Printer-friendly Version

Interactive Discussion



Modelling wave–current interactions off the east coast of Scotland

A. D. Sabatino et al.

Title Page

Abstract

Introduction

Conclusions

References

Tables

Figures

◀

▶

◀

▶

Back

Close

Full Screen / Esc

Printer-friendly Version

Interactive Discussion



- Bretherton, F. P. and Garrett, C. J.: Wavetrains in inhomogeneous moving media, *P. Roy. Soc. Lond. A Mat.*, 302, 529–554, 1968. 3106
- Bryden, I. G. and Couch, S. J.: ME1 marine energy extraction: tidal resource analysis, *Renew. Energ.*, 31, 133–139, 2006. 3102
- 5 Cavaleri, L., Bertotti, L., Torrisi, L., Bitner-Gregersen, E., Serio, M., and Onorato, M.: Rogue waves in crossing seas: the Louis Majesty accident, *J. Geophys. Res.-Oceans*, 117, 1–8, 2012. 3101
- Chawla, A. and Kirby, J. T.: Experimental study of wave breaking and blocking on opposing currents, *Coast. Engin. Proc.*, 1, 759–772, 1998. 3102
- 10 Chawla, A. and Kirby, J. T.: Monochromatic and random wave breaking at blocking points, *J. Geophys. Res.-Oceans*, 107, 4–1, 2002. 3102
- Codiga, D. L.: Unified tidal analysis and prediction using the UTide Matlab functions, Graduate School of Oceanography, University of Rhode Island Narragansett, RI, 2011. 3108
- Davies, A., Sauvel, J., and Evans, J.: Computing near coastal tidal dynamics from observations and a numerical model, *Cont. Shelf. Res.*, 4, 341–366, doi:10.1016/0278-4343(85)90047-0, 1985. 3102
- 15 Deardorff, J.: On the magnitude of the subgrid scale eddy coefficient, *J. Comput. Phys.*, 7, 120–133, 1971. 3105
- Dee, D., Uppala, S., Simmons, A., Berrisford, P., Poli, P., Kobayashi, S., Andrae, U., Balsameda, M., Balsamo, G., Bauer, P., Bechtold, P., Beljaars, A. C. M., van de Berg, L., Bidlot, J., Bormann, N., Delsol, C., Dragani, R., Fuentes, M., Geer, A. J., Haimberger, L., Healy, S. B., Hersbach, H., Hólm, E. V., Isaksen, L., Kållberg, P., Köhler, M., Matricardi, M., McNally, A. P., Monge-Sanz, B. M., Morcrette, J.-J., Park, B.-K., Peubey, C., de Rosnay, P., Tavolato, C., Thépaut, J.-N., and Vitart, F.: The ERA-Interim reanalysis: configuration and performance of the data assimilation system, *Q. J. Roy. Meteor. Soc.*, 137, 553–597, 2011. 3105, 3107, 3113
- 20 DHI: MIKE 3 Hydrodynamics User Manual, vol. 1, 2011a. 3104
- DHI: MIKE 21 Wave Modelling User Manual, vol. 1, 2011b. 3105
- Dietrich, G.: Die natürlichen Regionen von Nord-und Ostsee auf hydrographischer Grundlage, *Kieler Meeresforsch.*, 7, 35–69, 1950. 3102, 3104, 3111
- 30 Egbert, G. D., Erofeeva, S. Y., and Ray, R. D.: Assimilation of altimetry data for nonlinear shallow-water tides: quarter-diurnal tides of the Northwest European Shelf, *Cont. Shelf. Res.*, 30, 668–679, 2010. 3105

Modelling wave–current interactions off the east coast of Scotland

A. D. Sabatino et al.

Title Page

Abstract

Introduction

Conclusions

References

Tables

Figures

◀

▶

◀

▶

Back

Close

Full Screen / Esc

Printer-friendly Version

Interactive Discussion

- Ferziger, J. H. and Perić, M.: Computational Methods for Fluid Dynamics, vol. 3, Springer, Berlin, 2002. 3103
- Flather, R.: Estimates of extreme conditions of tide and surge using a numerical model of the north-west European continental shelf, *Estuar. Coast. Shelf S.*, 24, 69–93, 1987. 3102
- 5 Guedes Soares, C.: Representation of double-peaked sea wave spectra, *Ocean Eng.*, 11, 185–207, 1984. 3101, 3115
- Hasselmann, K.: On the spectral dissipation of ocean waves due to white capping, *Bound.-Lay. Meteorol.*, 6, 107–127, 1974. 3107
- Haver, S.: A possible freak wave event measured at the Draupner jacket January 1 1995, *Rogue waves 2004*, 1–8, 2004. 3101
- 10 Hearn, C., Hunter, J., and Heron, M.: The effects of a deep channel on the wind-induced flushing of a shallow bay or harbor, *J. Geophys. Res.-Oceans*, 92, 3913–3924, 1987. 3102
- Heath, M. R., Sabatino, A. D., Serpetti, N., and O’Hara Murray, R.: Scoping the impact tidal and wave energy extraction on suspended sediment concentrations and underwater light climate, *TeraWatt Position Papers, MASTS*, 2015. 3117
- 15 Huthnance, J.: Physical oceanography of the North Sea, *Ocean and Shoreline Management*, 16, 199–231, 1991. 3102
- Janssen, P. A. E. M.: Nonlinear four-wave interaction and freak waves, *J. Phys. Oceanogr.*, 33, 863–884, 2003. 3117
- 20 Johnson, H. K. and Kofoed-Hansen, H.: Influence of bottom friction on sea surface roughness and its impact on shallow water wind wave modeling, *J. Phys. Oceanogr.*, 30, 1743–1756, 2000. 3107
- Komen, G. J., Cavaleri, L., Donelan, M., Hasselmann, K., Hasselmann, S., and Janssen, P.: Dynamics and Modelling of Ocean Waves, Cambridge University Press, 1996. 3105, 3106, 3107
- 25 Lilly, D.: On the application of the eddy viscosity concept in the inertial sub-range of turbulence, NCAR Manuscript No. 123, National Center for Atmospheric Research, Boulder, CO, 1966. 3105
- Longuet-Higgins, M. S. and Stewart, R. W.: Radiation stress and mass transport in gravity waves, with application to “surf beats”, *J. Fluid Mech.*, 13, 481–504, doi:10.1017/S0022112062000877, 1962. 3117
- 30 Nikuradse, J.: Strömungsgesetze in rauhen Röhren, *Forschungsheft*, Volume 361, VDI-Verlag, 33 pp., 1933. 3107

Modelling wave–current interactions off the east coast of Scotland

A. D. Sabatino et al.

Title Page

Abstract

Introduction

Conclusions

References

Tables

Figures

◀

▶

◀

▶

Back

Close

Full Screen / Esc

Printer-friendly Version

Interactive Discussion



Onorato, M., Osborne, A., and Serio, M.: Modulational instability in crossing sea states: a possible mechanism for the formation of freak waves, *Phys. Rev. Lett.*, 96, 014503, doi:10.1103/PhysRevLett.96.014503, 2006. 3101

Onorato, M., Proment, D., and Toffoli, A.: Freak waves in crossing seas, *Eur. Phys. J.-Spec. Top.*, 185, 45–55, 2010. 3101

Osuna, P. and Monbaliu, J.: Wave–current interaction in the Southern North Sea, *J. Marine Syst.*, 52, 65–87, 2004. 3102

Otto, L., Zimmerman, J., Furnes, G., Mork, M., Saetre, R., and Becker, G.: Review of the physical oceanography of the North Sea, *Neth. J. Sea Res.*, 26, 161–238, 1990. 3102, 3104, 3111

Phillips, O. M.: *The Dynamics of the Upper Ocean*, 2nd edn., Cambridge University Press, Cambridge, London, New York, Melbourne, 1977. 3101

Ponce de León, S. and Guedes Soares, C.: Extreme wave parameters under North Atlantic extratropical cyclones, *Ocean Model.*, 81, 78–88, doi:10.1016/j.ocemod.2014.07.005, 2014. 3116, 3117

Proudman, J. and Doodson, A. T.: The principal constituent of the tides of the North Sea, *Philos. T. R. Soc. Lond.*, 224, 185–219, 1924. 3102

Ris, R. and Holthuijsen, L.: Spectral modelling of current induced wave-blocking, *Coast. Engin. Proc.*, 1, 1247–1254, 1996. 3102

Sabatino, A. D. and Serio, M.: Experimental investigation on statistical properties of wave heights and crests in crossing sea conditions, *Ocean Dynam.*, 65, 707–720, 2015. 3101

Serpetti, N., Heath, M., Armstrong, E., and Witte, U.: Blending single beam RoxAnn and multi-beam swathe QTC hydro-acoustic discrimination techniques for the Stonehaven area, Scotland, UK, *J. Sea Res.*, 65, 442–455, 2011. 3117

Serpetti, N., Heath, M., Rose, M., and Witte, U.: High resolution mapping of sediment organic matter from acoustic reflectance data, *Hydrobiologia*, 680, 265–284, 2012. 3117

Shields, M. A., Dillon, L. J., Woolf, D. K., and Ford, A. T.: Strategic priorities for assessing ecological impacts of marine renewable energy devices in the Pentland Firth (Scotland, UK), *Mar. Policy*, 33, 635–642, 2009. 3103

Shields, M. A., Woolf, D. K., Grist, E. P., Kerr, S. A., Jackson, A., Harris, R. E., Bell, M. C., Beharie, R., Want, A., Osalusi, E., Gibb, S. W., and Side, J.: Marine renewable energy: the ecological implications of altering the hydrodynamics of the marine environment, *Ocean Coast. Manage.*, 54, 2–9, 2011. 3103

**Modelling
wave–current
interactions off the
east coast of
Scotland**

A. D. Sabatino et al.

Title Page

Abstract

Introduction

Conclusions

References

Tables

Figures

◀

▶

◀

▶

Back

Close

Full Screen / Esc

Printer-friendly Version

Interactive Discussion



Signell, R. P., Beardsley, R. C., Graber, H., and Capotondi, A.: Effect of wave–current interaction on wind-driven circulation in narrow, shallow embayments, *J. Geophys. Res.-Oceans*, 95, 9671–9678, 1990. 3102, 3111

Smagorinsky, J.: General circulation experiments with the primitive equations: I. The basic experiment*, *Mon. Weather Rev.*, 91, 99–164, 1963. 3104, 3105

Song, Y. and Haidvogel, D.: A semi-implicit ocean circulation model using a generalized topography-following coordinate system, *J. Comput. Phys.*, 115, 228–244, 1994. 3104

Tamura, H., Waseda, T., and Miyazawa, Y.: Freakish sea state and swell-windsea coupling: numerical study of the Suwa-Maru incident, *Geophys. Res. Lett.*, 36, L01607, doi:10.1029/2008GL036280, 2009. 3101, 3117

Toffoli, A., Bitner-Gregersen, E., Osborne, A., Serio, M., Monbaliu, J., and Onorato, M.: Extreme waves in random crossing seas: laboratory experiments and numerical simulations, *Geophys. Res. Lett.*, 38, L06605, doi:10.1029/2011GL046827, 2011. 3101

Tolman, H. L.: Effects of tides and storm surges on North Sea wind waves, *J. Phys. Oceanogr.*, 21, 766–781, 1991. 3101

Toro, E. F.: *Riemann Solvers and Numerical Methods for Fluid Dynamics: A Practical Introduction*, Springer Science and Business Media, 2009. 3104

Venugopal, V. and Nimalidinne, R.: Marine Energy resource assessment for Orkney and Pentland waters with a coupled wave and tidal flow model, in: *ASME 2014 33rd International Conference on Ocean, Offshore and Arctic Engineering*, American Society of Mechanical Engineers, V09BT09A010–V09BT09A010, 2014. 3107, 3117

Venugopal, V. and Nimalidinne, R.: Wave resource assessment for Scottish waters using a large scale North Atlantic spectral wave model, *Renew. Energ.*, 76, 503–525, 2015. 3107, 3117

Waseda, T., Hallerstig, M., Ozaki, K., and Tomita, H.: Enhanced freak wave occurrence with narrow directional spectrum in the North Sea, *Geophys. Res. Lett.*, 38, L13605, doi:10.1029/2011GL047779, 2011. 3101

Whewell, W.: Essay towards a first approximation to a map of cotidal lines, *Abstracts of the papers printed in the Philos. T. Roy. Soc. Lond.*, 3, 188–190, 1830. 3102

Woolf, D. K., Challenor, P., and Cotton, P.: Variability and predictability of the North Atlantic wave climate, *J. Geophys. Res.-Oceans*, 107, 1–14, 2002. 3100

Xie, L., Liu, H., and Peng, M.: The effect of wave–current interactions on the storm surge and inundation in Charleston Harbor during Hurricane Hugo 1989, *Ocean Model.*, 20, 252–269, 2008. 3102

Young, I. R.: *Wind Generated Ocean Waves*, vol. 2, Elsevier, 1999. 3105

**Modelling
wave–current
interactions off the
east coast of
Scotland**

A. D. Sabatino et al.

Title Page

Abstract

Introduction

Conclusions

References

Tables

Figures



Back

Close

Full Screen / Esc

Printer-friendly Version

Interactive Discussion



Modelling wave–current interactions off the east coast of Scotland

A. D. Sabatino et al.

Table 1. Location of the validation/calibration instrumentation.

Description	Coordinates		Depth (m)	Used for
	longitude (°)	latitude (°)		
Aberdeen Tide Gauge	–2.0803	57.144	–	water level val/cal
Leith Tide Gauge	–3.1682	55.9898	–	water level validation
Buckie Tide Gauge	–2.9667	57.6667	–	water level validation
Firth of Forth buoy	–2.5038	56.1882	–	waves validation
Moray Firth buoy	–3.3331	57.9663	–	waves val/cal
Aberdeen wave rider	–2.0500	57.1608	–	waves validation
BODC 4551 RCM	–2.8000	57.7910	12	current validation
BODC 4561 RCM	–1.9680	57.2320	12	current validation
BODC 4562 RCM	–1.9680	57.2320	27	current validation
BODC 4571 RCM	–1.9020	57.2260	12	current validation
BODC 4572 RCM	–1.9020	57.2260	52	current validation
BODC 4582 RCM	–2.1500	56.9870	23	current validation
BODC 4591 RCM	–2.0980	56.9820	12	current validation
BODC 4592 RCM	–2.0980	56.9820	47	current validation

Title Page

Abstract

Introduction

Conclusions

References

Tables

Figures

◀

▶

◀

▶

Back

Close

Full Screen / Esc

Printer-friendly Version

Interactive Discussion

**Modelling
wave–current
interactions off the
east coast of
Scotland**

A. D. Sabatino et al.

Title Page

Abstract

Introduction

Conclusions

References

Tables

Figures

◀

▶

◀

▶

Back

Close

Full Screen / Esc

Printer-friendly Version

Interactive Discussion



Table 2. Computed RMS error for the main harmonic components, the validation for each tide gauge is reported in the Table S1 in the Supplement.

Components	RMS error	
	A (cm)	g (°)
M_2	2.52	0.78
S_2	1.64	3.68
N_2	1.31	3.02
O_1	0.76	5.42
K_1	0.44	14.4
Q_1	0.42	13.6

Modelling wave–current interactions off the east coast of Scotland

A. D. Sabatino et al.

Table 3. Results from the validation of the currents, showing the difference between the modelled and observed current speeds at the eight locations reported in Table 1.

RCM No	Lon	Lat	Depth (m)	RMSE (m s ⁻¹)	NRMSE	<i>R</i> ²	Bias (m s ⁻¹)
4551	-2.8	57.791	12	0.094	0.157	0.17	0.001
4561	-1.968	57.232	12	0.111	0.124	0.70	-0.03
4562	-1.968	57.232	27	0.075	0.105	0.75	-0.02
4571	-1.902	57.226	12	0.223	0.147	0.23	-0.05
4572	-1.902	57.226	52	0.087	0.112	0.80	-0.02
4582	-2.15	56.987	23	0.075	0.124	0.80	0.02
4591	-2.098	56.982	12	0.125	0.132	0.73	-0.062
4592	-2.098	56.982	47	0.073	0.121	0.82	-0.05

[Title Page](#)
[Abstract](#)
[Introduction](#)
[Conclusions](#)
[References](#)
[Tables](#)
[Figures](#)
[◀](#)
[▶](#)
[◀](#)
[▶](#)
[Back](#)
[Close](#)
[Full Screen / Esc](#)
[Printer-friendly Version](#)
[Interactive Discussion](#)


Modelling wave–current interactions off the east coast of Scotland

A. D. Sabatino et al.

Table 4. Wave gauges validation.

	Bias	Coupled			Bias	Uncoupled		
		RMSE	<i>R</i>	SI		RMSE	<i>R</i>	SI
Firth of Forth								
H_s	−0.02 m	0.30 m	0.941	0.27	−0.01 m	0.30 m	0.939	0.27
T_m	−0.70 s	1.17 s	0.767	0.25	−0.76 s	1.24 s	0.758	0.27
Moray Firth								
H_s	−0.14 m	0.42 m	0.849	0.38	−0.15 m	0.42 m	0.848	0.39
T_m	−1.18 s	1.75 s	0.668	0.39	−1.23 s	1.83 s	0.656	0.41
Aberdeen								
H_s	−0.07 m	0.21 m	0.836	0.32	−0.07 m	0.22 m	0.831	0.32
T_m	−0.25 s	0.91 s	0.715	0.20	−0.30 s	0.97 s	0.701	0.21
Satellite								
Winter								
H_s	−0.2 m	0.4 m	–	0.25	−0.2 m	0.4 m	–	0.25
T_m	+0 s	0.8 s	–	0.15	+0 s	0.8 s	–	0.15
Spring								
H_s	−0.1 m	0.3 m	–	0.21	−0.1 m	0.3 m	–	0.21
T_m	+0.1 s	1.2 s	–	0.23	+0.1 s	1.2 s	–	0.23

Modelling wave–current interactions off the east coast of Scotland

A. D. Sabatino et al.

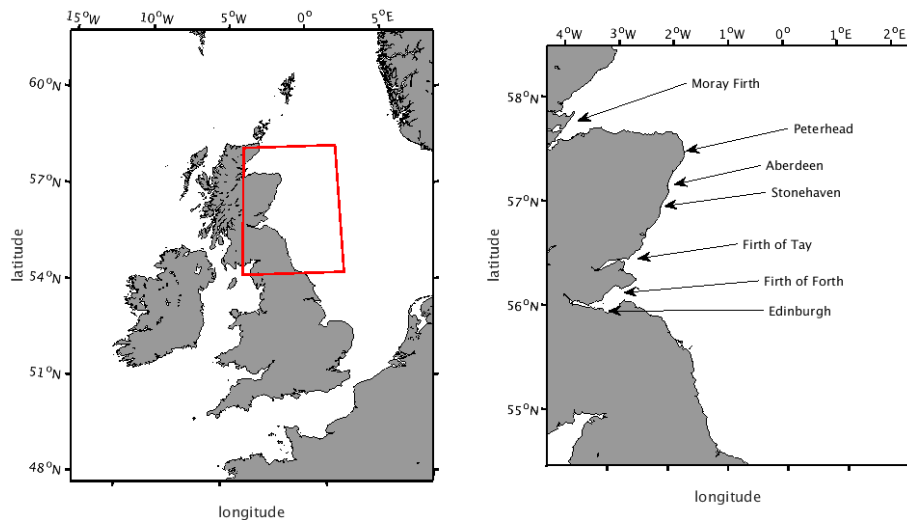


Figure 1. The area studied in the present paper.

Title Page

Abstract

Introduction

Conclusions

References

Tables

Figures

◀

▶

◀

▶

Back

Close

Full Screen / Esc

Printer-friendly Version

Interactive Discussion



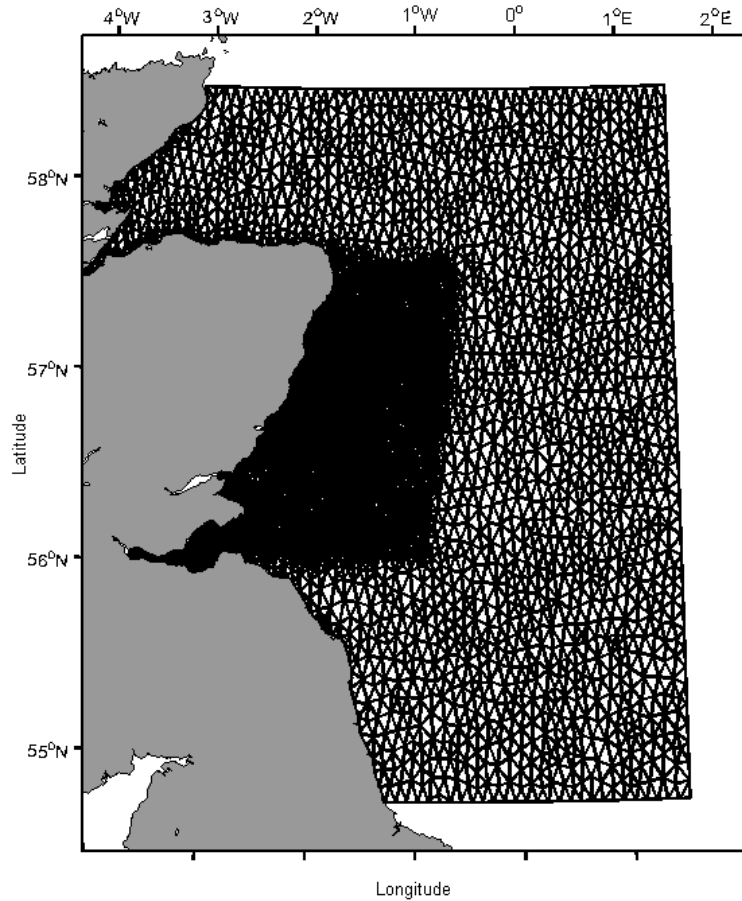


Figure 2. The computational grid generated with MIKE ZERO software.

**Modelling
wave–current
interactions off the
east coast of
Scotland**

A. D. Sabatino et al.

Title Page	
Abstract	Introduction
Conclusions	References
Tables	Figures
◀	▶
◀	▶
Back	Close
Full Screen / Esc	
Printer-friendly Version	
Interactive Discussion	



**Modelling
wave–current
interactions off the
east coast of
Scotland**

A. D. Sabatino et al.

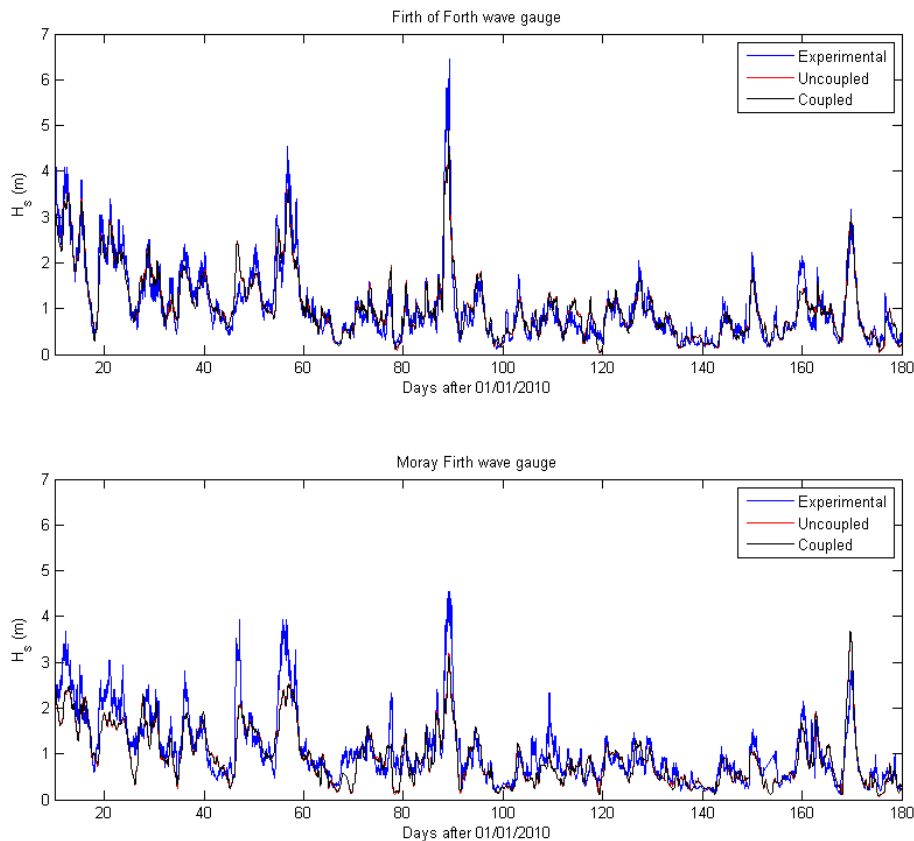


Figure 3. Comparison between experimental and modelled H_s in the Firth of Forth and in the Moray Firth for 2010.

Title Page

Abstract

Introduction

Conclusions

References

Tables

Figures

◀

▶

◀

▶

Back

Close

Full Screen / Esc

Printer-friendly Version

Interactive Discussion

Modelling wave–current interactions off the east coast of Scotland

A. D. Sabatino et al.

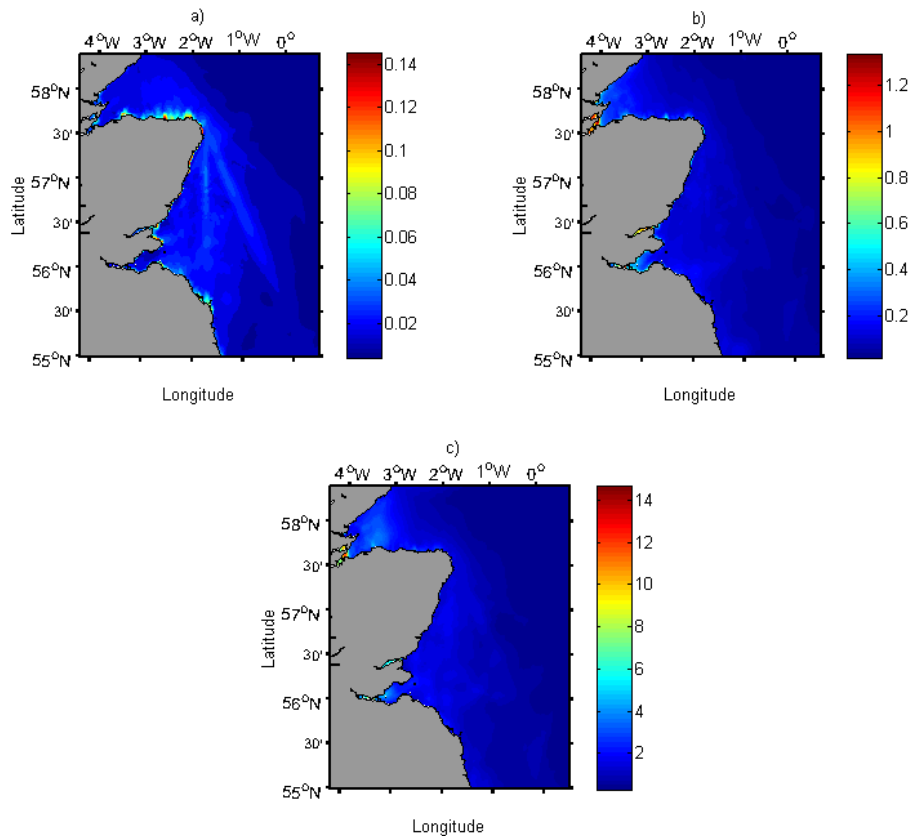


Figure 4. Root mean square difference between wave model output with and without WCI: **(a)** significant wave height (m), **(b)** peak wave period (s), **(c)** wave direction (degrees).

[Title Page](#)[Abstract](#)[Introduction](#)[Conclusions](#)[References](#)[Tables](#)[Figures](#)[◀](#)[▶](#)[◀](#)[▶](#)[Back](#)[Close](#)[Full Screen / Esc](#)[Printer-friendly Version](#)[Interactive Discussion](#)

Modelling wave–current interactions off the east coast of Scotland

A. D. Sabatino et al.

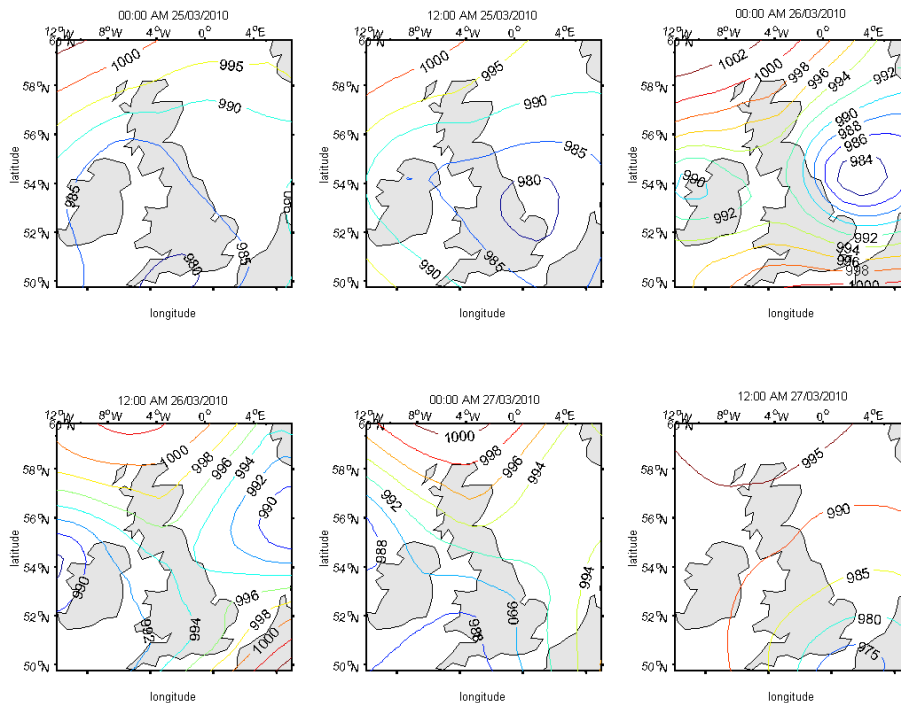


Figure 5. The mean sea level pressure fields (hPa) before and during the 25–26 February 2010 storm.

Modelling wave–current interactions off the east coast of Scotland

A. D. Sabatino et al.

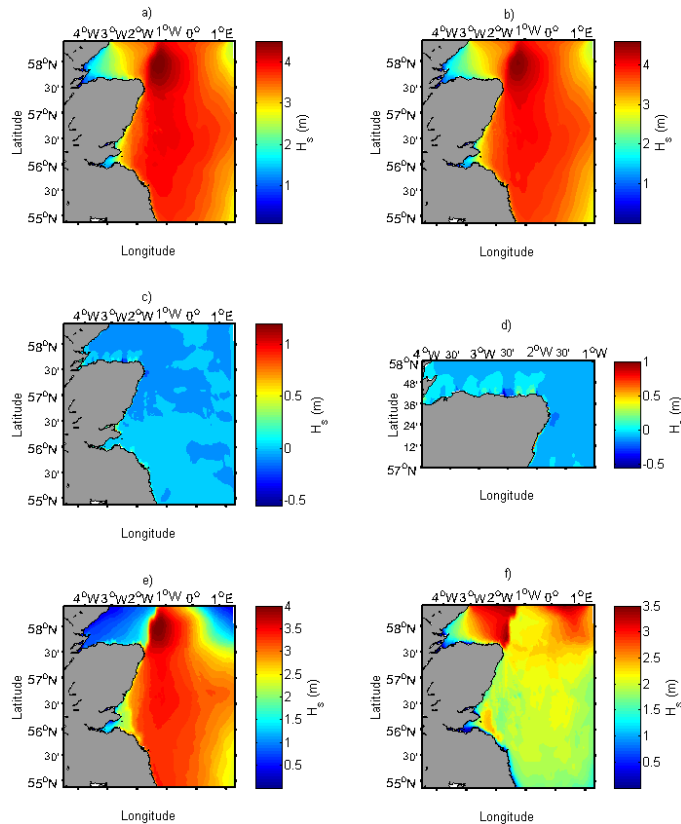


Figure 6. The modelled H_s in the east coast of Scotland at 12:30 UTC of the 26 February 2010: **(a)** coupled model (WCI on), **(b)** uncoupled model (WCI off), **(c)** difference between coupled and uncoupled, **(d)** difference between coupled and uncoupled in the Moray Firth area, **(e)** wind-sea waves, **(f)** swell waves.

Modelling wave–current interactions off the east coast of Scotland

A. D. Sabatino et al.

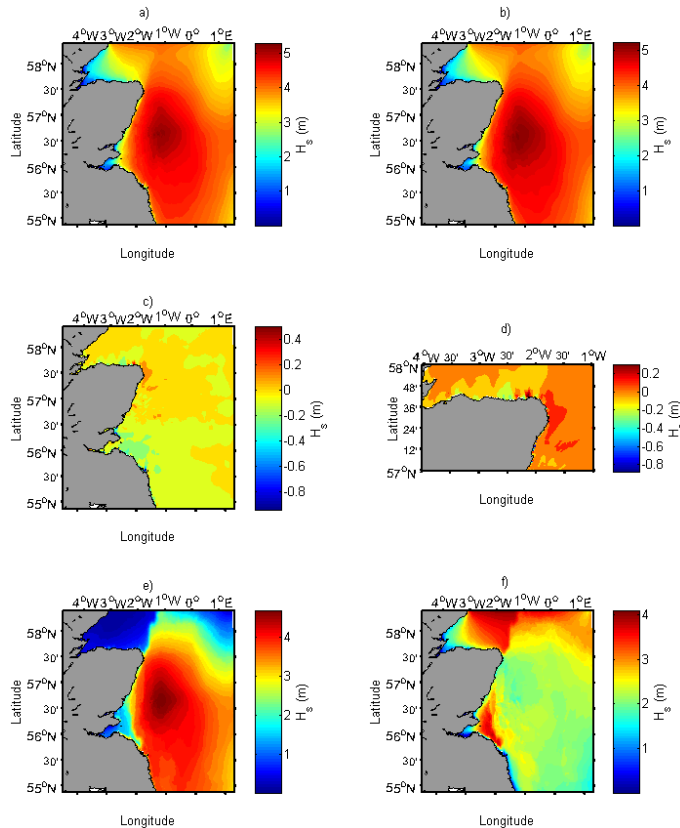


Figure 7. The modelled H_s in the east coast of Scotland at 19:00 UTC of the 26 February 2010: **(a)** coupled model (WCI on), **(b)** uncoupled model (WCI off), **(c)** difference between coupled and uncoupled, **(d)** difference between coupled and uncoupled in the Moray Firth area, **(e)** wind-sea waves, **(f)** swell waves.

Modelling wave–current interactions off the east coast of Scotland

A. D. Sabatino et al.

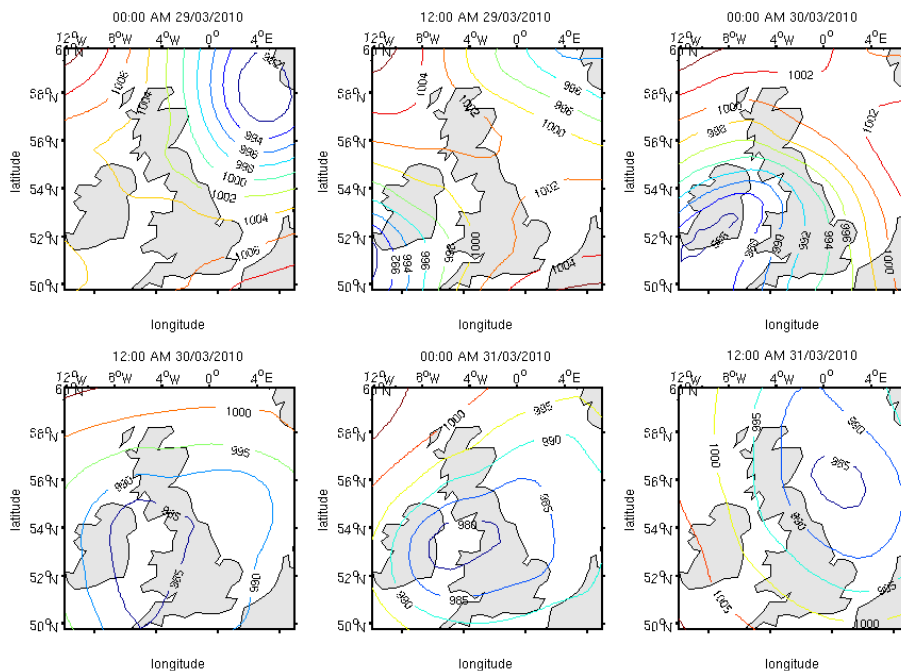


Figure 8. The mean sea level pressure fields (hPa) before and during the 30–31 March 2010 storm.

Modelling wave–current interactions off the east coast of Scotland

A. D. Sabatino et al.

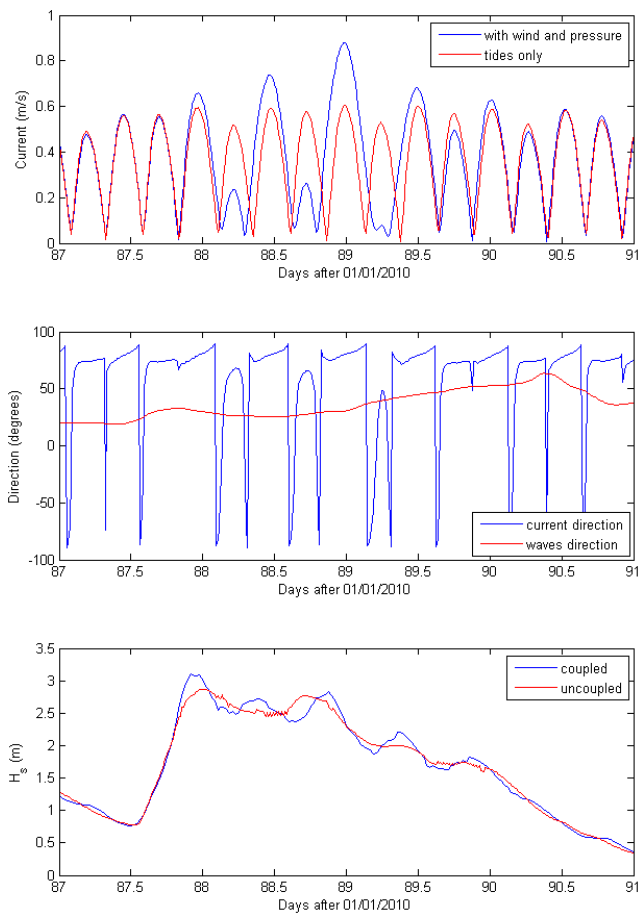


Figure 9. Modelled currents and waves conditions during the 30–31 March 2010 storm.

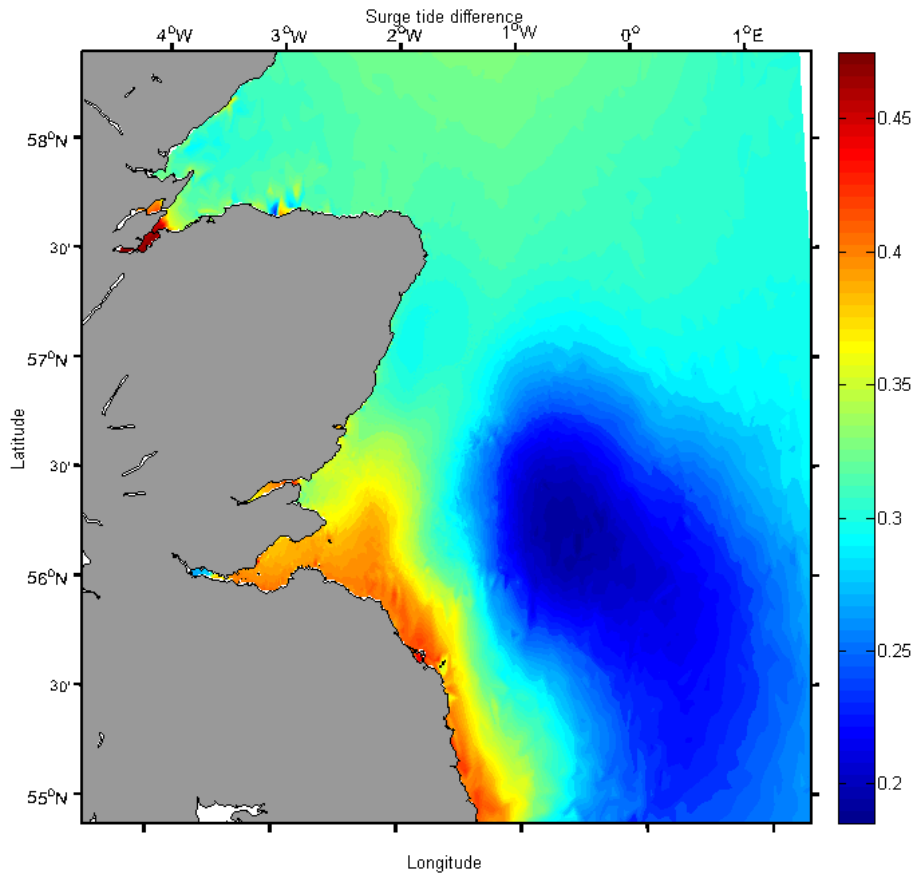


Figure 10. The surge wave at 02:00 UTC of the 31 March 2010.

**Modelling
wave–current
interactions off the
east coast of
Scotland**

A. D. Sabatino et al.

Title Page

Abstract

Introduction

Conclusions

References

Tables

Figures

◀

▶

◀

▶

Back

Close

Full Screen / Esc

Printer-friendly Version

Interactive Discussion



Modelling wave–current interactions off the east coast of Scotland

A. D. Sabatino et al.

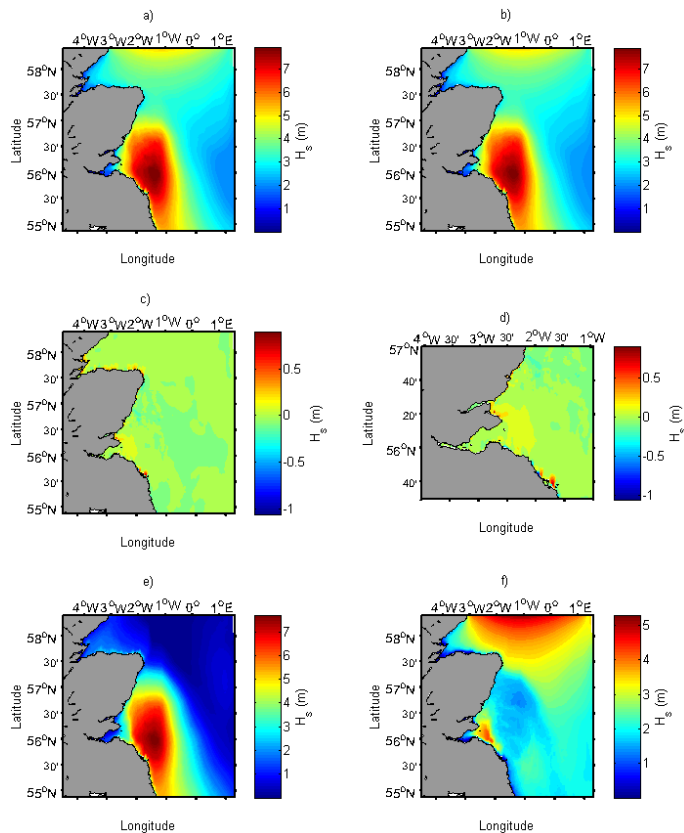


Figure 11. The modelled H_s in the east coast of Scotland at 00:30 UTC of the 31 March 2010: **(a)** coupled model (WCI on), **(b)** uncoupled model (WCI off), **(c)** difference between coupled and uncoupled, **(d)** difference between coupled and uncoupled in the Firth of Forth area, **(e)** wind-sea waves, **(f)** swell waves.

[Title Page](#)
[Abstract](#)
[Introduction](#)
[Conclusions](#)
[References](#)
[Tables](#)
[Figures](#)
[Back](#)
[Close](#)
[Full Screen / Esc](#)
[Printer-friendly Version](#)
[Interactive Discussion](#)

Modelling wave–current interactions off the east coast of Scotland

A. D. Sabatino et al.

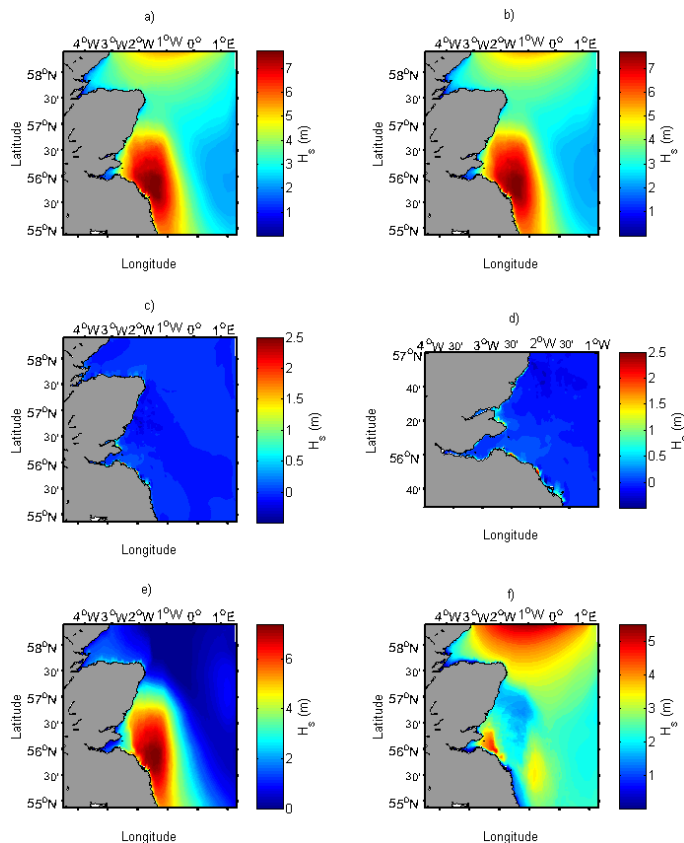


Figure 12. The modelled H_s in the east coast of Scotland at 02:00 UTC of the 31 March 2010: **(a)** coupled model (WCI on), **(b)** uncoupled model (WCI off), **(c)** difference between coupled and uncoupled, **(d)** difference between coupled and uncoupled in the Firth of Forth area, **(e)** wind-sea waves, **(f)** swell waves.

[Title Page](#)
[Abstract](#)
[Introduction](#)
[Conclusions](#)
[References](#)
[Tables](#)
[Figures](#)
[Back](#)
[Close](#)
[Full Screen / Esc](#)
[Printer-friendly Version](#)
[Interactive Discussion](#)

Modelling wave–current interactions off the east coast of Scotland

A. D. Sabatino et al.

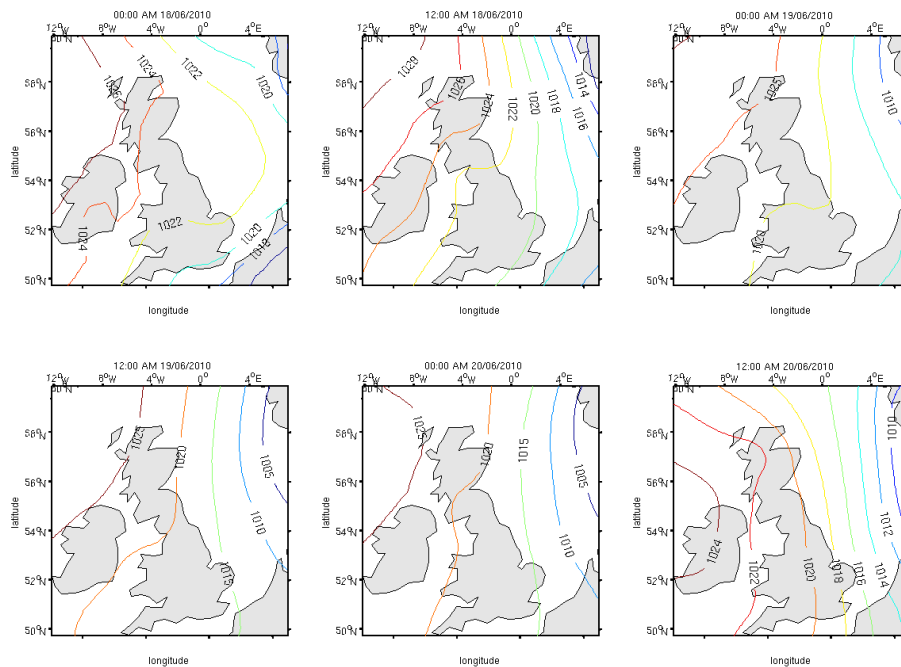


Figure 13. The mean sea level pressure fields (hPa) before and during the 19 June 2010 storm.

[Title Page](#)[Abstract](#)[Introduction](#)[Conclusions](#)[References](#)[Tables](#)[Figures](#)[◀](#)[▶](#)[◀](#)[▶](#)[Back](#)[Close](#)[Full Screen / Esc](#)[Printer-friendly Version](#)[Interactive Discussion](#)

Modelling wave–current interactions off the east coast of Scotland

A. D. Sabatino et al.

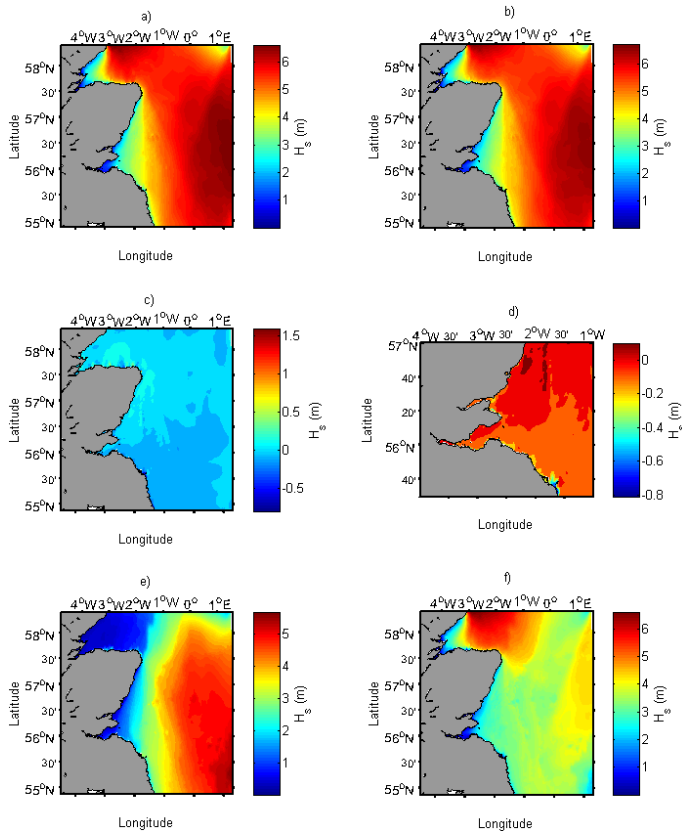


Figure 14. The modelled H_s in the east coast of Scotland at 16:00 UTC of the 19 June 2010: **(a)** coupled model (WCI on), **(b)** uncoupled model (WCI off), **(c)** difference between coupled and uncoupled, **(d)** difference between coupled and uncoupled in the Firth of Forth area, **(e)** wind-sea waves, **(f)** swell waves.

Modelling wave–current interactions off the east coast of Scotland

A. D. Sabatino et al.

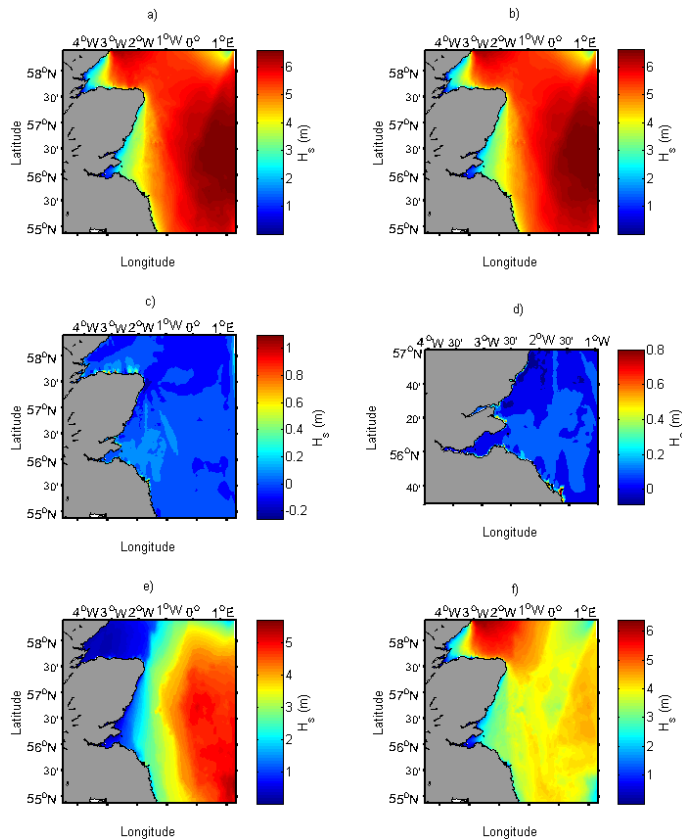


Figure 15. The modelled H_s in the east coast of Scotland at 19:00 UTC of the 19 June 2010: **(a)** coupled model (WCI on), **(b)** uncoupled model (WCI off), **(c)** difference between coupled and uncoupled, **(d)** difference between coupled and uncoupled in the Firth of Forth area, **(e)** wind-sea waves, **(f)** swell waves.